ACS OMEGA

Article

http://pubs.acs.org/journal/acsodf

Investigation of the Antibacterial Effect of Mesoporous Magnesium Carbonate

Ken Welch,* Mushtaq Ahmad Latifzada, Sara Frykstrand, and Maria Strømme*

Division of Nanotechnology and Functional Materials, Department of Engineering Sciences, The Ångström Laboratory, Uppsala University, Box 534, 751 21 Uppsala, Sweden

ABSTRACT: Mesoporous magnesium carbonate (MMC) was first presented in 2013, and this material is currently under consideration for use in a number of biotechnological applications including topical formulations. This study presents the first evaluation of the antibacterial properties of the material with mesoporous silica and two other magnesium-containing powder materials used as references. All powder materials in this study are sieved to achieve a particle size distribution between 25 and 75 μm. The Gram-positive bacterium *Staphylococcus epidermidis* is used as the model bacterium due to its prevalence on human skin, its likelihood of developing resistance to antibiotics, for example, from routine exposure to antibiotics secreted in sweat, and because it is found inside affected acne vulgaris pores. Quantification of bacterial viability using a metabolic activity assay with resazurin as the fluorescent indicator shows that MMC exerts a strong antibacterial effect on the bacteria and that alkalinity accounts for the major part of this effect. The results open up for further development of MMC in on-skin applications where bacterial growth inhibition without using antibiotics is deemed favorable.

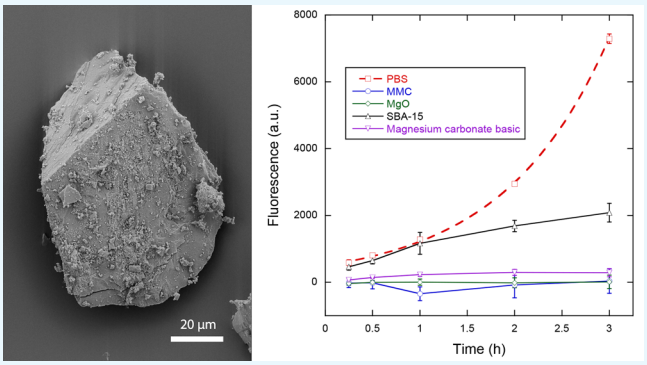

INTRODUCTION

About twice in a century, basic advances in science and technology bring about a total change in society, industry, and our everyday life. We are now beginning to approach the phase in which only incremental developments are to be expected from our latest major advance, the development of computers that has created a revolution in information and communication technology. Right now many indicators point toward the fact that advanced materials technology or nanotechnology will be the driver of the next science and technology revolution,[1−3] and the reason is that such technology has given us tools to decide which properties we want to give our materials. We are no longer at the mercy of the properties nature has given our materials but can instead start to precisely tailor them.

To exemplify, we have started to develop nanomaterial-based solar cells with the potential of outperforming those currently on the market by several hundred percent in efficiency, depending on significantly smaller amounts of material than in current solar cells,[4] nanostructured batteries based on sustainable materials such as cellulose and conducting polymers[5,6] or organic radical polymers,[7] targeted nanotechnology-based cancer treatments based on passive and active targeting of tumor cells,[8] and a number of other medicine inventions.[9] In spite of the great opportunity of nanotechnology within both energy technology and medicine, the cosmetics industry was among the first to implement nanotechnological principles in product development.[10] When it comes to skin care products based on nanotechnological principles, the borderline between cosmetics and medicine is thin. New nanostructures allow for delivery of both active pharmaceutical ingredients as well as purely cosmetic agents to different layers of the skin (topical) as well as through the skin (transdermal) to cause systemic effects.

Mesoporous nanomaterials constitute a very promising class of materials in such areas of use due to their tunable pore structure that can be adjusted to the ingredients to be loaded into, and subsequently released from, them. For example, such materials are presently evaluated for haircare,[10] dermal delivery of pharmaceutical compounds such as small interfering RNA to treat fibrosis,[11] and as delivery vehicles for peptides[12] and vitamins in cosmetic formulations.[13] The most frequently studied type of mesoporous material for such applications is mesoporous silica, whose synthesis typically relies on the use of organic template molecules[14,15] and relatively high calcination temperatures to create the desired pore structure.

In 2013, we presented the template-free synthesis of a mesoporous magnesium carbonate (MMC) material, commercialized as Upsalite,[16] that is synthesized in a low-temperature process and has a well-defined pore size distribution.[17] In addition to its ability to absorb a large amount of moisture,[16,18,19] this material has recently been found to be able to stabilize poorly soluble drugs incorporated into the mesopore structure of the material, thus enhancing their dissolution rate.[20,21] The material, which consists of amorphous

Received: July 14, 2016
Accepted: October 21, 2016
Published: November 14, 2016

DOI: 10.1021/acsomega.6b00124
ACS Omega 2016, 1, 907−914

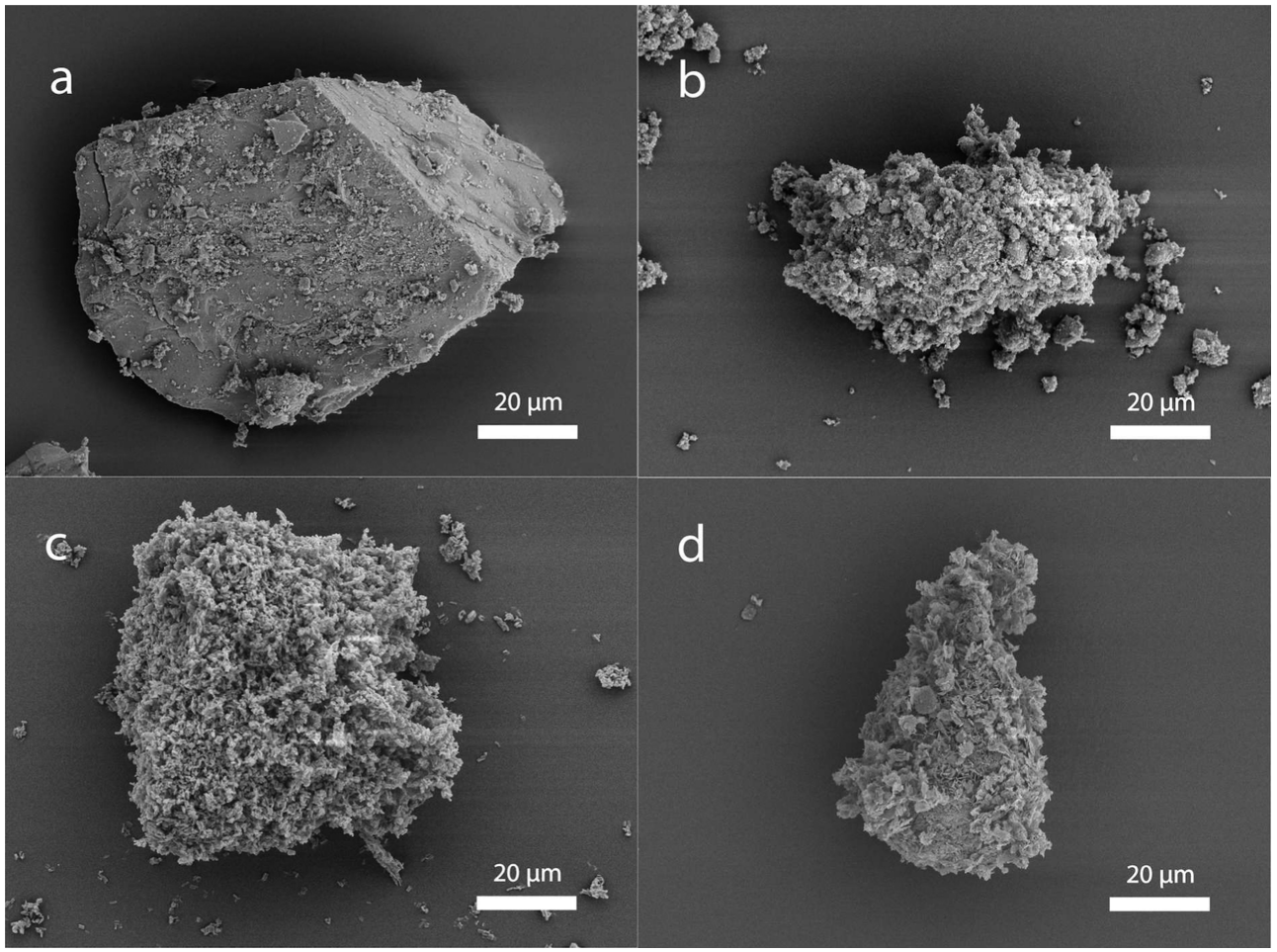

Figure 1. SEM images of a sieved sample particle of (a) MMC, (b) MgO, (c) SBA-15, and (d) magnesium carbonate basic.

magnesium carbonate and a small portion of crystalline magnesium oxide, has further been indicated to be safe to use on skin as it, even at very high concentrations, was shown to be nontoxic for human dermal fibroblast cells and to not induce cutaneous reactions in in vivo skin irritation tests. In addition, no evidence of systemic toxicity was found when saline extracts of the material were injected in mice.[22]

The above findings spur us to further investigate biomedical, and in particular on-skin, application areas of use for MMC. In this work, we present the first analysis of the antibacterial properties of this material and compare them with those of mesoporous silica and two other magnesium-containing powder materials to elucidate the mechanism of the observed properties. The Gram-positive bacterium *Staphylococcus epidermidis* is used as a model in this study due to its prevalence on human skin and also due to its likelihood of developing resistance to antibiotics, for example, from routine exposure to antibiotics secreted in sweat.[23] In addition, the bacterium is found inside affected acne vulgaris pores.[24]

RESULTS

Characterization of Sample Particles. Figure 1 displays scanning electron microscopy (SEM) images of a sieved particle from each of the four materials included in this study. Particles of MMC were generally single pieces of material corresponding in size to the sieved interval 25−75 μm, whereas particles of the three other materials consist of aggregates of much smaller primary particles.

Antibacterial Test. The antibacterial effect of MMC in comparison to magnesium oxide, mesoporous silica, and magnesium carbonate basic was assessed with the help of the metabolic activity assay (MAA) containing the metabolic indicator resazurin. The fluorescence of the assay containing the samples and bacteria provides a measure of the viability of the bacteria when corrected for the background fluorescence of the samples without bacteria. Figure 2 displays the fluorescence signals and thus the viability of the bacteria in contact with the four powder samples, as well as the viability of the negative control containing phosphate-buffered saline (PBS) without any powder. The PBS measurement was taken from the well with the highest bacterial concentration in the standard curve, which was identical to the bacteria concentration used with all powder samples. Measurements of the standard curve (not displayed) showed good linearity between fluorescence levels and bacteria concentrations at all measurement times.

The viability measurements of bacteria in PBS indicate a relatively uninhibited growth, as can be seen by the exponential increase in fluorescence measurements. An exponential fit to the data provides a generation or doubling time of the bacteria of $\ln(2)/0.897$ h $\approx$ 46 min. Both MMC and MgO indicate a strong antibacterial effect against *S. epidermidis*. Magnesium carbonate basic also shows a strong effect, albeit not to the same degree as MMC and MgO. Mesoporous silica does not

DOI: 10.1021/acsomega.6b00124
ACS Omega 2016, 1, 907−914

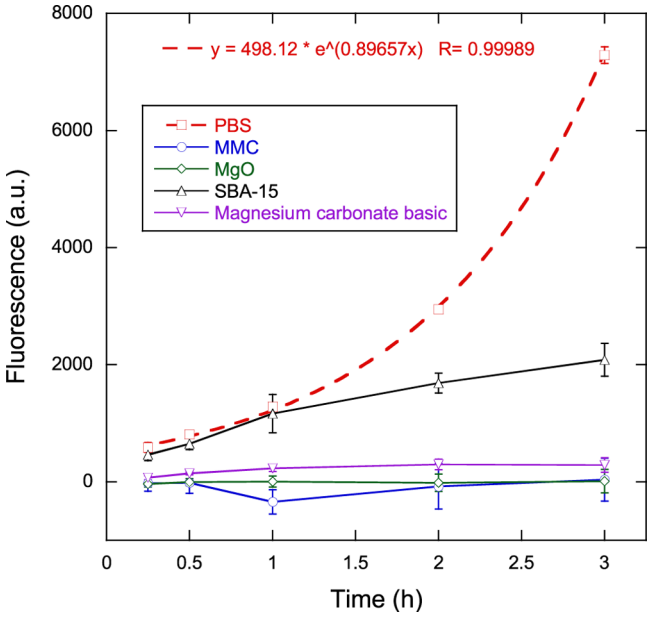

Figure 2. Viability measurements as a function of time for bacteria in contact with MMC, magnesium oxide, mesoporous silica, and magnesium carbonate basic in comparison to the negative control PBS. Solid lines are guides to the eye, whereas the dashed line represents an exponential fit to the data for PBS. Data represent mean ± 1 sd for $n = 3$.

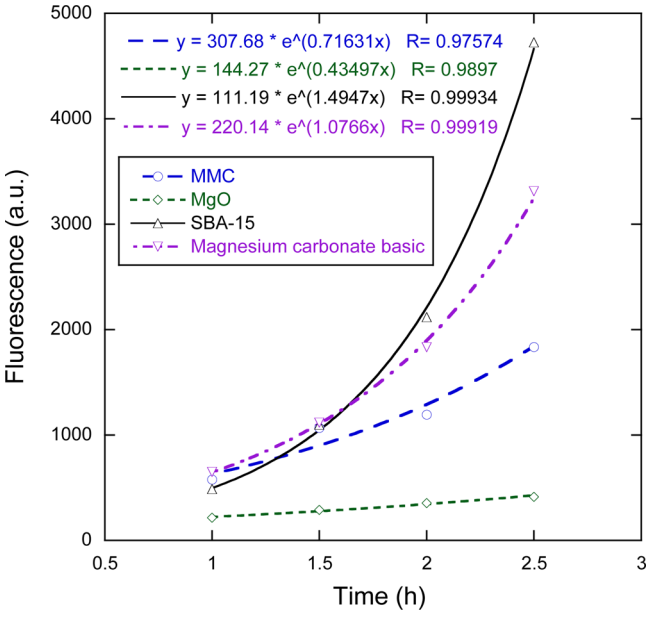

Figure 3. Fluorescence measurements showing the growth of bacteria suspensions after separation from the powder samples at the end of the antibacterial test. The legend indicates which sample powder the bacteria had previously been in contact with. Lines represent exponential fits to the data, with corresponding equations provided in the top left corner of the plot.

show any effect for the first hour compared to PBS, but subsequent measurements show an effect that reduced the bacterial growth/viability compared to PBS. After 3 h, the viability reductions compared to PBS were 71, 96, 100, and 100% for SBA-15, magnesium carbonate basic, MgO, and MMC, respectively.

Recovery Test. Results from the antibacterial test shown above indicate a strong antibacterial effect and/or growth inhibition for three of the materials tested. To determine whether the bacteria were completely inactivated, a recovery test was carried out where the bacteria were first separated from the powder suspension and MAA solution, and then reintroduced into a fresh MAA without sample particles. Figure 3 shows the growth curves of the bacteria that were previously subjected to the antibacterial test. All samples show some degree of viability, indicating that the bacteria were not completely killed during the antibacterial test, despite the fact that the viability reduction was nearly complete for MgO and MMC (see Figure 2). Generally, the rate of growth, indicated by the increasing levels of fluorescence in Figure 3, appears to correspond to the degree of viability reduction observed in the antibacterial test. The fluorescence levels are the lowest for MgO, suggesting that the antibacterial effect of MgO was the strongest. Although the viability of the bacteria in contact with MMC was at least as low as that for MgO in the previous test, the bacteria appear to have recovered to a greater extent when removed from contact with MMC. This suggests that although MMC completely inhibited the growth of *S. epidermidis*, it did not completely kill the bacteria.

Exponential curves are fitted to the data in Figure 3, and the corresponding equations can also be found in the plot. It is interesting to note that the generation time of the bacteria previously in contact with the SBA-15 powder was shorter than the generation time of bacteria that had not been in contact with any powder in the previous antibacterial test (28 min versus 46 min; see the PBS sample in Figure 2). This could likely be explained by the higher concentration of the Mueller–Hinton (MH) broth that was used in the MAA for the recovery test that consequently led to a higher growth rate.

Effect of Media pH. To investigate the effect of pH on the viability of *S. epidermidis*, the pH of the MAA media was adjusted between 7.4 and 10.5 by the addition of NaOH, and the fluorescence was measured after 30 min. Figure 4 displays the results of the test where the relative viabilities of the

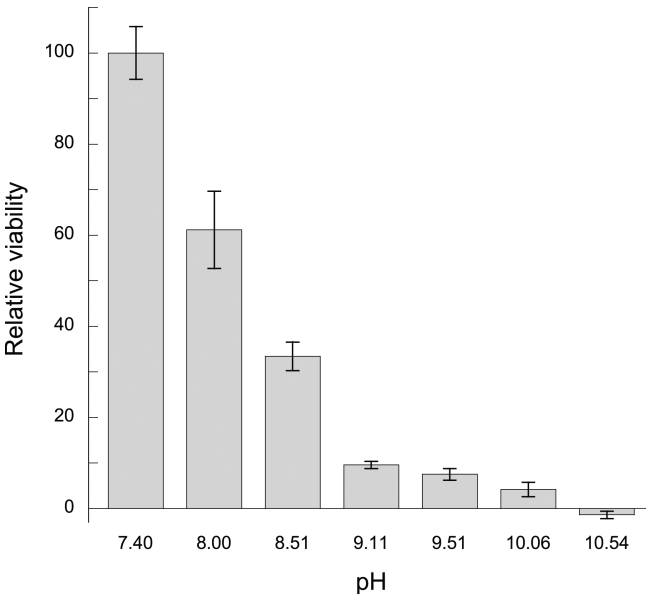

Figure 4. Relative viability of bacterial suspensions at pH ranging from 7.4 to 10.54, referenced to the viability of the unadjusted media at pH = 7.4. Data represent mean ± 1 sd for $n = 3$.

DOI: 10.1021/acsomega.6b00124
ACS Omega 2016, 1, 907–914

bacterial suspensions are shown relative to the unadjusted MAA media at pH = 7.4. It can be seen that a more alkaline environment reduces the viability of *S. epidermidis* or at least suppresses the growth; 90% viability/growth reduction is achieved with a pH of 9.11, whereas complete inhibition is observed at pH = 10.54.

Controlling for Effects of Media pH and Particles. An additional antibacterial test was performed with MMC, SBA-15, and MgO with the aim to separate antibacterial effects due to contact with the particles themselves from the effects due to possible substances leached from the materials. The test was performed in a MAA with sufficient buffer capacity to maintain the pH despite the presence of the basic materials being tested. This buffer capacity was verified by measuring the pH of the MAA solution containing the different sample powders over 4 h, which proved to be 7.25 ± 0.02, 7.10 ± 0.02, and 7.34 ± 0.02 for MMC, SBA-15, and MgO, respectively. This contrasts with the pH of the MAA solution containing the powders in the first antibacterial test, where the pH was found to be 8.39, 7.32, and 9.76 for MMC, SBA-15, and MgO, respectively.

Figure 5 displays the fluorescence signals, corresponding to the viability, of the bacteria in contact with the three powder samples, as well as that of the negative control containing PBS without any powder. As in the first antibacterial test detailed above, the PBS measurement corresponded to the well with the highest bacterial concentration in the standard curve, which was identical to the bacteria concentration used with all powder samples. Measurements of the standard curve (not displayed) showed good linearity between fluorescence levels and bacteria concentrations at all measurement times. Fluorescence signals were concurrently recorded on the bacteria suspensions placed in the filtered solutions in which the powder samples had previously been soaked. Differences between these fluorescence levels and the corresponding fluorescence levels from particle-containing wells were not statistically significant (unpaired Student *t*-test, $p > 0.05$), and thus, only the fluorescence measurements from the bacterial suspensions in contact with the sample particles are displayed.

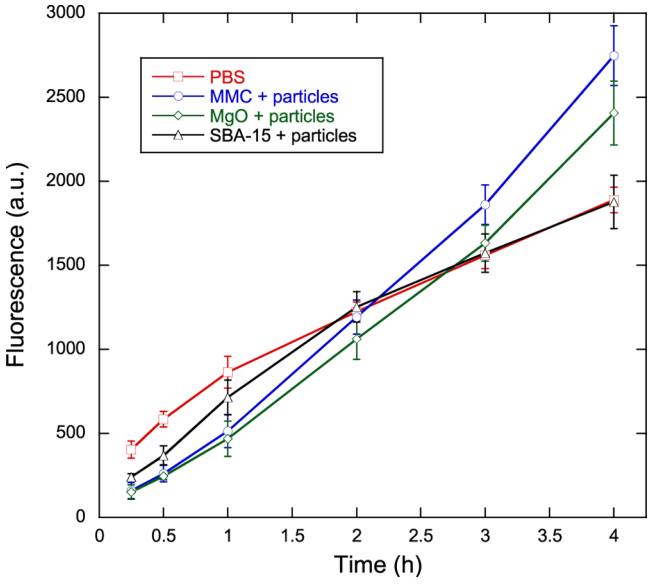

Figure 5. Viability measurements as a function of time for bacteria in contact with MMC, magnesium oxide, and mesoporous silica in concentrated PBS (phosphate concentration 0.3 M). A negative control without powder (denoted PBS) is provided for comparison. Solid lines are provided as guides to the eye. Data represent mean ± 1 sd for $n = 3$.

The growth behavior of bacteria in only PBS is markedly different from that shown in Figure 2 for only PBS. In Figure 5, the growth rate of bacteria in PBS decreases as the test proceeds instead of following the exponential profile observed in Figure 2. This can be attributed to the high ion concentration of concentrated PBS, making the medium hypertonic relative to the bacterial cells and leading to loss of water from the bacterial cells due to osmosis. On examining the fluorescence of the bacteria suspensions in contact with particles, there appears to be an initial viability reduction relative to the PBS sample after 15 min (61, 63, and 40% for MMC, MgO, and SBA-15, respectively), but after continued contact with the particles, the viability increases relative to the viability of bacteria in PBS. After approximately 2 h, the viability of the bacteria subjected to SBA-15 match and follow that of bacteria in PBS, whereas the viability of both MMC and MgO continues to grow linearly and exceeds the viability of bacteria in PBS by as much as 47% (for the bacteria in contact with MMC particles after 4 h).

DISCUSSION

In this study, MMC was investigated for antibacterial activity against *S. epidermidis*. Information about the bactericidal properties of this material is important for the development of applications, such as topical formulations. Equally important is obtaining information on the biocompatibility of this mesoporous material. Recently, MMC was subjected to a toxicological evaluation through in vitro cytotoxicity, skin irritation, and acute systemic toxicity in vivo tests.[22] These tests showed that the material was nontoxic for human dermal fibroblasts cells up to a concentration of 1 mg/mL after 48 h exposure and that topical application of MMC resulted in negligible cutaneous reactions.

It is clear from the antibacterial test (cf. Figure 2) that MMC exhibits strong antibacterial activity against *S. epidermidis* at a concentration of 1 mg/mL, resulting in essentially no bacterial viability during the entire three-hour test. Three possible mechanisms have been proposed for the antibacterial activity of materials similar to those used in this study, namely, direct interaction of particles with bacteria,[25−27] an alkaline effect,[28,29] and the formation of reactive oxygen species (ROS).[30−37]

Figure 4 proves that *S. epidermidis* bacteria are sensitive to an alkaline environment and therefore it is reasonable to expect some degree of alkaline effect from MMC because the addition of 1 mg/mL powder raised the pH of the MAA media to 8.39. The increase in pH with MMC is likely due to the residual MgO present in the material as previously shown.[17] However, from Figure 4 we would only expect approximately 65% reduction in viability with a media pH of 8.39, whereas Figure 2 shows a 100% viability reduction (although the bacteria are not permanently inactivated, as indicated by the recovery test shown in Figure 3). Therefore, the alkalinity of the MAA solution cannot entirely explain the antibacterial activity of MMC. With the MgO sample, which also resulted in a 100% viability reduction, the alkalinity of the MAA media (pH = 9.76) can explain a larger proportion of the antibacterial effect but still not all of it because Figure 4 indicates that a pH greater than 10 is required for complete viability reduction of *S. epidermidis*. A possible explanation for this increased antibacterial activity could be the increased pH of a thin layer of

DOI: 10.1021/acsomega.6b00124
ACS Omega 2016, 1, 907−914

water surrounding the particles that results in damage to the bacterial cell membrane when coming in contact with the particles.[28] The bacteria are more likely to come into contact with the particles if they are electrostatically attracted to each other. *S. epidermidis*, like most bacteria, carry a net negative surface charge under typical physiological conditions[38] and thus would be attracted to positively charged substrates in the media. The isoelectric point (IEP) for MgO is around 12,[39] which means that it carries a positive charge in media with a pH less than 12 and would attract the negatively charged *S. epidermidis*. Previously, the surface charge of MgO nanoparticles has been determined to be positive, and thus attractive, to both Gram-positive and Gram-negative bacteria.[27] A similar situation may exist for MMC because it contains some residual MgO, although the IEP for the crystalline form of magnesium carbonate, magnesite, is only 6.8.[40] In the case of SBA-15 particles, another mechanism must be responsible for the viability reduction because this material did not alter the pH of the MAA media, and its IEP is around 3.6,[41] meaning it would be negatively charged in the media.

Interaction between bacteria and particles in direct contact with them is another mechanism of antibacterial activity. As discussed above, particles can be electrostatically attracted to bacteria due to their surface charge and the subsequent absorption can damage the cell membrane,[25−27] and perhaps the particles can even enter the interior of the cells.[25] Typically, this occurs with nanoparticles where smaller particles show increased antibacterial activity.[25,26] In the current study, all samples were sieved to a 25−75 μm particle (or aggregate) size distribution, and therefore, such direct interaction between the particles and bacteria was not expected to be as great as it would be if the particles or aggregates were nanosized. However, for samples other than MMC, particles consist of aggregates of much smaller primary particles, where at least one dimension is on the order of 1 μm or less, as can be observed in Figure 1. It is highly likely that the mechanical agitation during testing caused some of these particles to break into smaller ones, which may have led to an increased antibacterial effect for these materials. The diameter of the *S. epidermidis* bacteria used in this study is just under 1 μm[42] and therefore it is possible that the smaller primary particles of some sample materials may interact strongly with the bacteria, or perhaps even enter into the bacteria, and cause an antibacterial effect. This would not be the case for MMC in which the particles are clearly not composed of smaller primary nanoparticles.

The third possible mechanism to the antibacterial activity is the generation of ROS, such as the superoxide ion (O_2^-). For example, several studies have shown that MgO particles generate superoxide ions[30−33] and that a larger surface area increases the effect. This may be applicable in the case of MMC particles, which have a surface area of 207 m^2/g. It has also been shown that SBA-15 particles at a concentration of 1 mg/mL generate superoxide ions that cause cytotoxic effects on Caco-2 cells.[43] The specific surface area of SBA-15 was previously measured to be 428 m^2/g.[22] Thus, it is likely that generation of ROS is responsible for the antibacterial effect of SBA-15 observed in this study. Similarly, the high surface area of MMC particles, which also contain some residual MgO, suggests that ROS provide a significant contribution to the observed antibacterial effect.

Finally, we return to the results where attempts to control the effects of media pH and particles were made. As described above, a major contributor to the antibacterial activity is deemed to be the increased alkalinity of the MAA media, at least in the case of MMC and MgO particles. By increasing the buffer capacity of the MAA solution, the pH for all samples was the same as the PBS reference, and thus, the effect of alkalinity was removed. Figure 5 showed that no sample material had a viability that was reduced compared to the PBS reference (in fact MMC and MgO had increased viability levels after 3 h compared to the PBS reference). However, as discussed above, alkalinity effects of the MAA media should not have accounted for the entire antibacterial effect. As such, some effect of the particles was also expected, but this was not observed because there was no statistical difference between the results with or without particles. A likely explanation for this lack of effect seen with particles compared to without particles is the electrostatic screening caused by the very high ion concentration of the phosphate buffer (0.3 M). This screening would likely decrease the attraction and thus interaction between particles and bacteria, and consequently reduce effects due to direct contact, ROS generation, or local pH increase close to the particle surface.

In summary, alkalinity accounts for the major part of MMC's antibacterial activity toward *S. epidermidis*, although it cannot entirely explain the effect. Other contributions to this antibacterial effect are likely due to the generation of ROS such as O_2^-, direct contact with the particles, and/or an increased pH in close proximity to the particles. Future studies should be directed at elucidating the mechanisms behind the antibacterial activity, as well as determining this activity against other bacterial strains and microorganisms. For example, it is known that oxides like MgO and ZnO are more effective against Gram-positive than Gram-negative bacteria[36] and that the susceptibility to alkalinity and ROS varies with bacteria strain.

METHODS

Sample Preparation and Characterization. Synthesis of MMC (Upsalite) was carried out as described previously,[22] with the exception that the material was ground in a mortar to reduce the particle size and thereafter sieved to obtain a powder with a particle size distribution between 25 and 75 μm. The material had a surface area of 207 m^2/g, a pore volume of 0.34 cm^3/g, an average pore size of 5.3 nm, and a density of 2.28 g/cm^3. Details of the characterization can be found elsewhere.[22]

Three other materials were included in the study: mesoporous silica (SBA-15; ACS Material, LLC); magnesium oxide (MgO, CAS no. 1309-48-4; Sigma-Aldrich); and magnesium carbonate basic (CAS no. 39409-82-0; Sigma-Aldrich). All powders were sieved to achieve a particle size distribution between 25 and 75 μm.

Before testing, all powder samples were sterilized by heating to 180 °C for 3 h.[44]

Characterization of particle size was performed with a scanning electron microscope (Leo 1550 SEM; Zeiss, Oberkochen, Germany), operating at an acceleration voltage of 5 keV. Sieved powders were first sputter coated with a thin layer of gold/palladium to minimize charging effects.

Bacterial Strain. The bacterial strain *Staphylococcus epidermidis* (CCUG 18 000A) was used for all experiments. MH Broth (Sigma-Aldrich, Steinheim, Germany) was used to inoculate *S. epidermidis* overnight at 37 °C, after which the bacteria were centrifuged (1500*g*, 10 min, EBA 30 centrifuge; Hettich, Tuttlingen, Germany), collected, and resuspended in 250 μL of sterilized PBS (Product no P4417; Sigma-Aldrich).

DOI: 10.1021/acsomega.6b00124
ACS Omega 2016, 1, 907−914

The concentration of bacteria was adjusted to an optical density (OD_{600}) of 0.6 (UV spectrophotometer, UV-1800; Shimadzu), corresponding to approximately 6×10^8 CFU/mL.

MAA. Quantification of bacterial viability was performed using a MAA with resazurin as the fluorescent indicator. In the assay, blue nonfluorescent resazurin is reduced to pink, fluorescent resorufin by metabolic intermediates, resulting in fluorescence being a sensitive indicator of viable bacteria.[45]

To perform the MAA, wells in a 48-well plate were first filled with 200 μL of sterilized MH broth, 50 μL of resazurin solution at a concentration of 100 μg/mL, and 150 μL of PBS containing the sample to be tested. Immediately before viability testing, 100 μL of bacterial suspension in PBS at an OD of 0.06 was added to the well and thoroughly mixed with a pipette tip. The well plate was then placed in an orbital shaking incubator at 37 °C with shaking set to 250 rpm to limit settling of the particle samples and to increase bacteria−sample contact. At specific time points, the well plate was removed from the incubator, and fluorescence measurements were made in a microplate reader (Tecan Infinite M200), set to 530 nm excitation and 590 nm emission.

To check for linearity of the fluorescence readings with known concentrations of bacteria, three standard curves were recorded in parallel with each experiment. The standard curve consisted of a dilution series of nine wells containing 100 μL of bacterial suspension from OD = 0.06 to 0.003, 200 μL of sterilized MH broth, 200 μL of sterilized PBS, and resazurin at a concentration of 10 μg/mL.

Antibacterial Test. Suspensions of each powder to be tested (MMC, MgO, magnesium carbonate basic, and SBA-15) at a concentration of 1 mg/mL were used in the MAA for the antibacterial testing. Measurements were made in triplicate. Additionally, three wells containing each sample material, but without bacteria, were tested to determine the background fluorescence level of the MAA solutions/suspensions. Bacterial viability was determined as the difference in fluorescence levels between the wells with and without bacteria. Fluorescence measurements were made at 15, 30 min, and 1−3 h.

Recovery Test. To determine whether bacteria were permanently inactivated during the antibacterial test, a subsequent recovery test was performed where the bacteria were isolated from the sample powders and media used in the antibacterial test. This was accomplished by first allowing the powders to settle to the bottom of the wells for 5 min following the final fluorescence measurement after 3 h of bacteria−sample contact. Then, 100 μL of bacterial suspension from the upper half of each of the three sample wells was extracted and placed in a 1.5 mL centrifuge tube. The procedure was repeated for a second 1.5 mL centrifuge tube to which an additional 300 μL of ethanol was added to ensure that the bacteria were killed. For each sample material, both tubes were then centrifuged (1500*g*, 10 min, EBA 30 centrifuge; Hettich, Tuttlingen, Germany), and the supernatant was poured out. Bacteria were resuspended in MH broth and resazurin (10 μg/mL) and another MAA was performed with fluorescence measurements made at 1, 1.5, 2, and 2.5 h. The difference in fluorescence levels between the bacteria with and without added ethanol provided the viability of the bacteria after the antibacterial test when separated from the powder suspensions.

Effect of Media pH. The effect of pH on the growth of *S. epidermidis* was investigated by performing the MAA with media prepared at pH from 7.4 to 10.5, adjusted by the addition of NaOH. Six wells at each pH level were tested, three with bacteria and three without. The difference in fluorescence signal after 30 min of incubation at 37 °C provided the measure of bacterial viability.

Controlling for Effects of Media pH and Particles. An additional antibacterial test was performed using a concentrated PBS, with increased buffer capacity to maintain the pH at approximately 7.4 in the presence of the added powder samples. Additionally, to separate antibacterial effects due to contact with the particles themselves from the effects due to possible substances leached from the materials, testing of the media in which the sample powders had previously been soaked was carried out in parallel with testing of the media containing particles. Specifically, 100 mg of sample powder was added to 30 mL of 1.0 M PBS and placed in a tube rotator for 16 h. Subsequently, half of the suspension was centrifuged (1500*g*, 10 min, EBA 30 centrifuge; Hettich, Tuttlingen, Germany) and the supernatant was filtered through a 0.45 μm cellulose acetate membrane to remove any remaining particles. Both filtered PBS and PBS containing particle suspensions were tested using the MAA. When combined with the other constituents of the MAA, the resulting phosphate concentration was 0.3 M, and where applicable the particle concentration was 1 mg/mL. Three samples of both groups (filtered or particle-containing) of each material (MMC, MgO, or SBA-15) were tested with fluorescence readings made at 15, 30 min, 1−4 h. As in the Antibacterial section described above, additional three wells for both groups of each material, but without bacteria, were tested to determine the background fluorescence level of the MAA solutions/suspensions. Bacterial viability was determined as the difference in fluorescence levels between the wells with and without bacteria. Finally, pH measurements of the MAA solution containing the different sample powders were made at 0, 2, 3, and 4 h to determine any changes in the media pH.

AUTHOR INFORMATION

Corresponding Authors

*E-mail: ken.welch@angstrom.uu.se (K.W.).
*E-mail: maria.stromme@angstrom.uu.se (M.S.).

Notes

The authors declare the following competing financial interest(s): M.S. and S.F. are co-founders of Disruptive Materials, a company that performs R&D on MMC.

ACKNOWLEDGMENTS

This work was supported by the Swedish Research Council (VR).

REFERENCES

(1) Paull, R.; Wolfe, J.; Hebert, P.; Sinkula, M. Investing in nanotechnology. *Nat. Biotechnol.* **2003**, *21*, 1144−7.

(2) Silberglitt, R.; Anton, P. S.; Howell, D. R.; Wong, A.; Gassman, N.; Jackson, B. A.; Landree, E.; Pfleeger, S. L.; Newton, E. M.; Wu, F. *The Global Technology Revolution 2020, In-Depth Analyses: Bio/Nano/Materials/Information Trends, Drivers, Barriers, and Social Implications*; RAND Corporation: Santa Monica, CA, 2006. http://www.rand.org/pubs/technical_reports/TR303.html (accessed Sept 1, 2016)

(3) Nolan, A.; Pilat, D. Benefiting from the Next Production Revolution, 2016. http://oecdinsights.org/2016/02/23/benefiting-from-the-next-production-revolution/ (accessed Sept 1, 2016)

(4) Kempa, T. J.; Day, R. W.; Kim, S. K.; Park, H. G.; Lieber, C. M. Semiconductor nanowires: a platform for exploring limits and concepts for nano-enabled solar cells. *Energy Environ. Sci.* **2013**, *6*, 719−733.

DOI: 10.1021/acsomega.6b00124
ACS Omega 2016, 1, 907−914

(5) Nyholm, L.; Nyström, G.; Mihranyan, A.; Strømme, M. Toward Flexible Polymer and Paper-Based Energy Storage Devices. *Adv. Mater.* **2011**, *23*, 3751−3769.
(6) Wang, Z.; Carlsson, D. O.; Tammela, P.; Hua, K.; Zhang, P.; Nyholm, L.; Strømme, M. Surface Modified Nanocellulose Fibers Yield Conducting Polymer-Based Flexible Supercapacitors with Enhanced Capacitances. *ACS Nano* **2015**, *9*, 7563−71.
(7) Nakahara, K.; Oyaizu, K.; Nishide, H. Organic Radical Battery Approaching Practical Use. *Chem. Lett.* **2011**, *40*, 222−227.
(8) Wicki, A.; Witzigmann, D.; Balasubramanian, V.; Huwyler, J. Nanomedicine in cancer therapy: Challenges, opportunities, and clinical applications. *J. Controlled Release* **2015**, *200*, 138−157.
(9) Fadeel, B.; Kasemo, B.; Malmsten, M.; Strømme, M. Nanomedicine: reshaping clinical practice. *J. Intern. Med.* **2010**, *267*, 2−8.
(10) Mihranyan, A.; Ferraz, N.; Strømme, M. Current status and future prospects of nanotechnology in cosmetics. *Prog. Mater. Sci.* **2012**, *57*, 875−910.
(11) Morry, J.; Ngamcherdtrakul, W.; Gu, S. D.; Goodyear, S. M.; Castro, D. J.; Reda, M. M.; Sangvanich, T.; Yantasee, W. Dermal delivery of HSP47 siRNA with NOX4-modulating mesoporous silica-based nanoparticles for treating fibrosis. *Biomaterials* **2015**, *66*, 41−52.
(12) Kilpeläinen, M.; Riikonen, J.; Vlasova, M. A.; Huotari, A.; Lehto, V. P.; Salonen, J.; Herzig, K. H.; Järvinen, K. In vivo delivery of a peptide, ghrelin antagonist, with mesoporous silicon microparticles. *J. Controlled Release* **2009**, *137*, 166−70.
(13) Canham, L. Porous Silicon for Oral Hygiene and Cosmetics. In *Handbook of Porous Silicon*; Canham, L., Ed.; Springer International Publishing: Cham, 2014; pp 1−8.
(14) Widenmeyer, M.; Anwander, R. Pore size control of highly ordered mesoporous silica MCM-48. *Chem. Mater.* **2002**, *14*, 1827−1831.
(15) Yamada, T.; Zhou, H. S.; Asai, K.; Honma, I. Pore size controlled mesoporous silicate powder prepared by triblock copolymer templates. *Mater. Lett.* **2002**, *56*, 93−96.
(16) Forsgren, J.; Frykstrand, S.; Grandfield, K.; Mihranyan, A.; Strømme, M. A Template-Free, Ultra-Adsorbing, High Surface Area Carbonate Nanostructure. *PLoS One* **2013**, *8*, No. e68486.
(17) Frykstrand, S.; Forsgren, J.; Mihranyan, A.; Strømme, M. On the pore forming mechanism of Upsalite, a micro- and mesoporous magnesium carbonate. *Microporous Mesoporous Mater.* **2014**, *190*, 99−104.
(18) Pochard, I.; Frykstrand, S.; Ahlström, O.; Forsgren, J.; Strømme, M. Water and ion transport in ultra-adsorbing porous magnesium carbonate studied by dielectric spectroscopy. *J. Appl. Phys.* **2014**, *115*, No. 044306.
(19) Pochard, I.; Frykstrand, S.; Eriksson, J.; Gustafsson, S.; Welch, K.; Strømme, M. Dielectric Spectroscopy Study of Water Behavior in Calcined Upsalite: A Mesoporous Magnesium Carbonate without Organic Surface Groups. *J. Phys. Chem. C* **2015**, *119*, 15680−15688.
(20) Zhang, P.; Forsgren, J.; Strømme, M. Stabilisation of amorphous ibuprofen in Upsalite, a mesoporous magnesium carbonate, as an approach to increasing the aqueous solubility of poorly soluble drugs. *Int. J. Pharm.* **2014**, *472*, 185−191.
(21) Zhang, P.; Zardán Goméz De La Torre, T.; Forsgren, J.; Bergström, C. A. S.; Strømme, M. Diffusion-Controlled Drug Release from the Mesoporous Magnesium Carbonate Upsalite. *J. Pharm. Sci.* **2016**, *105*, 657−663.
(22) Frykstrand, S.; Forsgren, J.; Zhang, P.; Strømme, M.; Ferraz, N. Cytotoxicity, in Vivo Skin Irritation and Acute Systemic Toxicity of the Mesoporous Magnesium Carbonate Upsalite. *J. Biomater. Nanobiotechnol.* **2015**, *6*, 257−266.
(23) Høiby, N.; Jarlov, J. O.; Kemp, M.; Tvede, M.; Bangsborg, J. M.; Kjerulf, A.; Pers, C.; Hansen, H. Excretion of ciprofloxacin in sweat and multiresistant *Staphylococcus epidermidis*. *Lancet* **1997**, *349*, 167−9.
(24) Bek-Thomsen, M.; Lomholt, H. B.; Kilian, M. Acne is not associated with yet-uncultured bacteria. *J. Clin. Microbiol.* **2008**, *46*, 3355−60.
(25) Makhluf, S.; Dror, R.; Nitzan, Y.; Abramovich, Y.; Jelinek, R.; Gedanken, A. Microwave-assisted synthesis of nanocrystalline MgO and its use as a bacteriocide. *Adv. Funct. Mater.* **2005**, *15*, 1708−1715.
(26) Pan, X.; Wang, Y.; Chen, Z.; Pan, D.; Cheng, Y.; Liu, Z.; Lin, Z.; Guan, X. Investigation of Antibacterial Activity and Related Mechanism of a Series of Nano-Mg(OH)2. *ACS Appl. Mater. Interfaces* **2013**, *5*, 1137−1142.
(27) Stoimenov, P. K.; Klinger, R. L.; Marchin, G. L.; Klabunde, K. J. Metal oxide nanoparticles as bactericidal agents. *Langmuir* **2002**, *18*, 6679−6686.
(28) Sawai, J.; Kojima, H.; Igarashi, H.; Hashimoto, A.; Shoji, S.; Takehara, A.; Sawaki, T.; Kokugan, T.; Shimizu, M. Escherichia coli damage by ceramic powder slurries. *J. Chem. Eng. Jpn.* **1997**, *30*, 1034−1039.
(29) Yamamoto, O.; Sawai, J.; Sasamoto, T. Change in antibacterial characteristics with doping amount of ZnO in MgO-ZnO solid solution. *Int. J. Inorg. Mater.* **2000**, *2*, 451−454.
(30) Hewitt, C. J.; Bellara, S. R.; Andreani, A.; Nebe-Von-Caron, G.; McFarlane, C. M. An evaluation of the anti-bacterial action of ceramic powder slurries using multi-parameter flow cytometry. *Biotechnol. Lett.* **2001**, *23*, 667−675.
(31) Huang, L.; Li, D.; Lin, Y.; Evans, D. G.; Duan, X. Influence of nano-MgO particle size on bactericidal action against *Bacillus subtilis* var. niger. *Chin. Sci. Bull.* **2005**, *50*, 514−519.
(32) Huang, L.; Li, D. Q.; Lin, Y. J.; Wei, M.; Evans, D. G.; Duan, X. Controllable preparation of Nano-MgO and investigation of its bactericidal properties. *J. Inorg. Biochem.* **2005**, *99*, 986−993.
(33) Krishnamoorthy, K.; Manivannan, G.; Kim, S. J.; Jeyasubramanian, K.; Premanathan, M. Antibacterial activity of MgO nanoparticles based on lipid peroxidation by oxygen vacancy. *J. Nanopart. Res.* **2012**, *14*, No. 1063.
(34) Yamamoto, O.; Fukuda, T.; Kimata, M.; Sawai, J.; Sasamoto, T. Antibacterial characteristics of MgO-mounted spherical carbons prepared by carbonization of ion-exchanged resin. *J. Ceram. Soc. Jpn.* **2001**, *109*, 363−365.
(35) Yamamoto, O.; Ohira, T.; Alvarez, K.; Fukuda, M. Antibacterial characteristics of $CaCO_3$-MgO composites. *Mater. Sci. Eng. B* **2010**, *173*, 208−212.
(36) Sawai, J.; Kojima, H.; Igarashi, H.; Hashimoto, A.; Shoji, S.; Sawaki, T.; Hakoda, A.; Kawada, E.; Kokugan, T.; Shimizu, M. Antibacterial characteristics of magnesium oxide powder. *World J. Microbiol. Biotechnol.* **2000**, *16*, 187−194.
(37) Sawai, J.; Shiga, H.; Kojima, H. Kinetic analysis of death of bacteria in CaO powder slurry. *Int. Biodeterior. Biodegrad.* **2001**, *47*, 23−26.
(38) Rawlinson, L. A.; O'Gara, J. P.; Jones, D. S.; Brayden, D. J. Resistance of *Staphylococcus aureus* to the cationic antimicrobial agent poly(2-(dimethylamino ethyl)methacrylate) (pDMAEMA) is influenced by cell-surface charge and hydrophobicity. *J. Med. Microbiol.* **2011**, *60*, 968−76.
(39) Carter, C. B.; Norton, M. G. Coatings and Thick Films. In *Ceramic Materials: Science and Engineering*, 2nd ed.; Springer Science +Business Media: New York, 2013; p 502.
(40) Gence, N.; Ozbay, N. pH dependence of electrokinetic behavior of dolomite and magnesite in aqueous electrolyte solutions. *Appl. Surf. Sci.* **2006**, *252*, 8057−8061.
(41) Vinu, A.; Murugesan, V.; Hartmann, M. Adsorption of lysozyme over mesoporous molecular sieves MCM-41 and SBA-15: Influence of pH and aluminum incorporation. *J. Phys. Chem. B* **2004**, *108*, 7323−7330.
(42) Unosson, E.; Morgenstern, M.; Engqvist, H.; Welch, K. In vitro antibacterial properties and UV induced response from *Staphylococcus epidermidis* on Ag/Ti oxide thin films. *J. Mater. Sci.: Mater. Med.* **2016**, *27*, 49.
(43) Heikkilä, T.; Santos, H. A.; Kumar, N.; Murzin, D. Y.; Salonen, J.; Laaksonen, T.; Peltonen, L.; Hirvonen, J.; Lehto, V. P. Cytotoxicity study of ordered mesoporous silica MCM-41 and SBA-15 microparticles on Caco-2 cells. *Eur. J. Pharm. Biopharm.* **2010**, *74*, 483−494.

DOI: 10.1021/acsomega.6b00124
ACS Omega 2016, 1, 907−914

(44) WHO. Essential Medicines and Health Products, Methods of Sterilization. In *The International Pharmacopoeia*, 5th ed. [Online]; WHO, 2015. http://apps.who.int/phint/alt/index.html#d/b.7.5.9 (accessed Sept 1, 2016).
(45) Sarker, S. D.; Nahar, L.; Kumarasamy, Y. Microtitre plate-based antibacterial assay incorporating resazurin as an indicator of cell growth, and its application in the in vitro antibacterial screening of phytochemicals. *Methods* **2007**, *42*, 321−4.

DOI: 10.1021/acsomega.6b00124
ACS Omega 2016, 1, 907−914